Zootaxa 5831 (1): 019–034
https://www.mapress.com/zt/

Article

ISSN 1175-5326 (print edition)
ZOOTAXA
ISSN 1175-5334 (online edition)

https://doi.org/10.11646/zootaxa.5831.1.2
http://zoobank.org/urn:lsid:zoobank.org:pub:F3D895CC-99DE-4FE1-9FE9-801C9A5E489E

A new species of *Diplacanthopoma* (Teleostei: Bythitidae) from the western Atlantic, with comments on the discovery and description of larval forms of two western Atlantic species

MATTHEW G. GIRARD[1,*], TIMO MORITZ[2] & WERNER SCHWARZHANS[3,4]
[1]*Department of Vertebrate Zoology, National Museum of Natural History, Smithsonian Institution, Washington, DC 20560, USA.*
GirardMG@si.edu; https://orcid.org/0000-0003-3580-6808
[2]*Leibniz Institute for the Analysis of Biodiversity Change, Hamburg, Germany.*
t.moritz@leibniz-lib.de; https://orcid.org/0000-0003-1281-7432
[3]*Natural History Museum of Denmark, University of Copenhagen, Universitetsparken 15, DK-2100 Copenhagen, Denmark.*
[4]*Ahrensburger Weg 103, D-22359 Hamburg, Germany.*
wwschwarz@aol.com; https://orcid.org/0000-0003-4842-7989
[*]*Corresponding author*

Abstract

The tropical and subtropical genus of viviparous cusk-eels *Diplacanthopoma* (Teleostei: Bythitidae) is differentiated from other bythitids in having a naked head, a fleshy flap bearing a large sensory pore above the opercle, and a large sensory pore on the cheek. The sensory pore on the cheek (i.e., "*Diplacanthopoma*" pore) is only known from two genera of ophidiiforms, *Diplacanthopoma* and *Hephthocara. Diplacanthopoma* includes eight nominal species, with seven in the Indian or Pacific Oceans, and one, *D. brachysoma*, from the western Atlantic. Recently, blackwater SCUBA divers collected two elongate larval fishes off West Palm Beach, Florida. Fin-ray and vertebral/myomere counts and DNA sequence data support the identification of one of the larvae as *D. brachysoma*; the first time the larval form for this genus of fishes has been identified. The second larva has higher numbers of medial-fin rays (184 dorsal-fin rays, 140 anal-fin rays) than *D. brachysoma* (125–164 dorsal-fin rays and 88–127 anal-fin rays), and mitochondrial cytochrome *c* oxidase subunit 1 barcode divergence of >9%, indicating the presence of a second undescribed species of *Diplacanthopoma* from the western Atlantic Ocean. We found three specimens (one from southern Brazil and two from the Bay of Campeche) in the Leibniz Institute for the Analysis of Biodiversity Change and the Smithsonian Institution's National Museum of Natural History fish collections that overlap in fin-ray and vertebral/myomere counts with the larval specimen from Florida. We describe this new species of *Diplacanthopoma* based on larval and adult characters. We also highlight intraspecific variation in counts and measurements for *D. brachysoma*, emphasizing further study is needed to understand the taxonomic diversity of this genus of the Bythitidae.

Key words: Brazil, Caribbean, COI, DNA barcodes, Deep-sea fishes

Introduction

Diplacanthopoma is a circumglobal genus of viviparous cusk-eels (Bythitidae) found in tropical and subtropical waters. Günther (1887) described the genus based on a single specimen caught off northern Brazil (*D. brachysoma*) and differentiated it from other bythitids by its characteristic stout opercular spines, with one spine directed posteriorly and another spine directed ventrally. Although not mentioned in the description, the ventrally directed spine is the ventral arm of the opercle that often pierces through the skin. The genus currently includes eight nominal species, seven from the Indian or Pacific Oceans, and only one, *D. brachysoma*, from the Atlantic (Nielsen *et al*. 1999; Fricke *et al*. 2025). *Diplacanthopoma alcocki* Goode & Bean, 1896 from the Indian Ocean is regarded as *nomen nudum* following the assessment of Cohen & Nielsen (2002). Despite this group being known for more than 135 years, species of *Diplacanthopoma* remain poorly characterized. Gosline's (1954: 70) assessment of the genus concluded that it was "impossible" to assess the validity of species, most had been "inadequately described," and variation

Accepted by K. Tang: 4 May 2026; published: 12 Jun. 2026

within nominal species of *Diplacanthopoma* "remains unknown" based on available specimens. These findings were likely due, in part, to the low number of specimens available and the scarcity of counts provided in previous species descriptions of *Diplacanthopoma*. Gosline (1954) and Machida (1988) provided counts and measurements of the specimens they examined but did not list comparable data for other known species of *Diplacanthopoma*. Cohen & Nielsen (2002) provided the most complete list of counts for holotypes or syntypes of five species. For the most common species in collections, *D. brachysoma*, Cohen & Nielsen (2002) listed 132 dorsal-fin rays, 98 anal-fin rays and 24 pectoral-fin rays for the holotype, all of which are more than what is shown in the specimen illustrated in Günther (1887, plate XXIII C; ~49 dorsal-fin rays, ~34 anal-fin rays, ~16 pectoral-fin rays). Cohen & Nielsen (2002) also noted that the slender tail section is often broken off or otherwise damaged in specimens of *Diplacanthopoma*, resulting in anomalously low fin-ray counts, caudal-vertebral counts, and standard-length measurements. Cohen & Nielsen (2002) highlighted that some specimens have a regenerated or healed caudal-fin region, adding to the uncertainty surrounding diagnostic counts and measurements for these fishes. Over the past ~70 years, more than 230 specimens have been identified and cataloged in collections as species of *Diplacanthopoma*, but there are more specimens identified to the genus level (i.e., *Diplacanthopoma*; *D.* sp.) than to a single described species (i.e., *D. brachysoma*; excluding specimens identified in this study; GBIF.org 2025). Although multiple authors have indicated additional undescribed species are present, including Gosline (1954; his "*D.* sp.?" from Hawaii) and Cohen & Haedrich (1983; their undescribed bythitid from the Galápagos hydrothermal vents), it remains difficult to assess the species diversity of these fishes without gaining an understanding of intraspecific variation in counts and measurements across species in the genus.

The recent popularity of blackwater diving and photography, in combination with community science and DNA-barcoding efforts, have allowed for new larval behaviors to be observed (Pastana *et al.* 2022; Afonso *et al.* 2025, Johnson *et al.* 2025), and larvae to be identified (e.g., Nonaka *et al.* 2021), particularly in the understudied order Ophidiiformes (Girard *et al.* 2023a, b, 2024). In 2021 and 2022, blackwater divers photographed and collected two large, elongate larvae off the coast of West Palm Beach, Florida. Upon examination of both phenotypic and genotypic characters, we identify these specimens as the larvae of *Diplacanthopoma*. We describe the larvae from this genus for the first time, identifying one larva as *D. brachysoma*. Based on the identification of more than 140 adult specimens of *D. brachysoma*, detailed examination of 24 of these specimens to understand intraspecific variation in fin-ray and vertebral counts, as well as comparisons of cytochrome *c* oxidase subunit 1 (COI) DNA barcode data, it is evident that the second larval specimen represents an undescribed western Atlantic species of *Diplacanthopoma*. During our investigation, we discovered three adult specimens that overlap in fin-ray and vertebral/myomere counts with the unidentified specimen. Based on DNA data from the larva, and comparisons of counts and measurements across larval and adult individuals, we describe a new, and second species, of *Diplacanthopoma* from the western Atlantic.

Materials and methods

Morphological identification, examination, and laboratory imaging of larvae and adults. Museum codes follow Sabaj (2020) except for NMNH referring to non-Fishes Division personnel and resources at the National Museum of Natural History, Smithsonian Institution, and LIB referring to non-Ichthyology personnel and resources at the Leibniz Institute for the Analysis of Biodiversity Change. We identified 149 specimens in 80 lots of adult *D. brachysoma* in the USNM collection (Supplementary S1). A subset of these specimens (24) was used for counts and measurements. All specimens used for counts and measurements, including their lengths, preparations, and museum catalog numbers, are listed in the Specimens Examined section below. Standard-length measurements of adult specimens were taken with a measuring tape to the nearest 1 mm. All other measurements of larval and adult specimens were taken with analog caliper to the nearest 0.1 mm. Larval and a subset of adult specimens were cleared and stained following Potthoff (1984) with the modifications listed in Girard *et al.* (2020) to examine internal osteology. All other specimens examined were X-rayed using either two-dimensional X-ray or three-dimensional microcomputed tomography (μCT) to view internal osteology. Two-dimensional X-rays were performed using Thermo Scientific PXS5-927 MicroFocus 90kV X-Ray Source and a duraSCAN 1417-NDI Digital Flat Panel X-Ray Detector at NMNH. Three-dimensional μCT scans were generated using either a YXLON FF20 CT at LIB, a Nikon Metrology XT H 225 ST at BMNH, or a GE Phoenix v|tome| x M 240/180kV Dual Tube μCT at NMNH. Scan settings were 80–110 kV, 140–201 μA, 250–500 ms exposure time, and 20–41 μm voxel size. Resulting

scans are available through MorphoSource project ID 000799225 and media identifiers as: 000799373 [USNM 407635], 000799649, 000799652 [BMNH 1887.1.2.7.54], 000803979, 000803982 [ZMH-ICH-0107333]. All scan data were visualized and segmented using the SlicerMorph module (Rolfe *et al.* 2021) in 3D Slicer (Fedorov *et al.* 2012) following the protocol described in Girard *et al.* (2022). All other specimen imaging was performed using equipment and protocols listed in Girard *et al.* (2020).

Abbreviations used for measurements (Table 1): **SL** = standard length; **D/A** = dorsal-fin ray that inserts over first anal-fin ray; **D/V** = first dorsal-fin ray that inserts over vertebra; **V/A** = anal-fin ray that inserts under vertebra; **HL** = head length; **HW** = head width; **HD** = head depth; **OL** = otolith length; **OH** = otolith height; **OT** = otolith thickness; **TCL** = sulcus length (measured as total colliculum length); **TCH** = sulcus height (measured as total colliculum height).

DNA extraction, amplification, and analysis. Protocols for tissue sampling, DNA extraction, amplification, and sequencing the barcode region of COI from larval specimens follow the methods described in Nonaka *et al.* (2021) and Weigt *et al.* (2012) using primers from Baldwin *et al.* (2009). Sequence contigs were built, edited, and assembled into FASTA files using Geneious Prime 2025.0.1 (Kearse *et al.* 2012). Sequences were deposited on GenBank, with the following accession numbers: PZ298823–PZ298825. Once generated, sequence data from larvae were aligned with barcode data generated from an adult specimen of *D. brachysoma* (USNM 407635; GenBank Nucleotide PZ298825). Measurements of sequence divergence were calculated by Geneious Prime as percentage of bases which are not identical based on the resulting sequence alignment. Additional mitochondrial data of *D. brachysoma* were identified (GenBank Nucleotide: AP004408, GenBank SRA: SRR16897167) and downloaded from GenBank but lacked identifiable museum voucher information. We do not make explicit comparisons between our data and these additional GenBank records in this study as we could not examine the associated voucher specimen(s).

Map generation. Distributions were mapped based on capture coordinates for specimens of *Diplacanthopoma* identified in this study (Supplementary S1). Coordinates were imported into QGIS-LTR vers. 3.16.6-Hannover and plotted over the following *Natural Earth* "Large Scale Vectors": Cultural Admin 0 –Boundary Lines land boundaries (vers. 5.1.0), Physical Bathymetry 0m (vers. 4.1.0), 200m (vers. 4.0.0), 1,000m (vers. 4.0.0), Physical Coastline (vers. 4.1.0).

Specimens used for counts and measurements. " * " following specimen count indicates specimen was µCT scanned. " ′ " following specimen count indicates specimen sequenced for COI. CS = cleared-and-stained specimen(s); EtOH = ethanol specimen(s). ***Diplacanthopoma brachysoma*:** BMNH 1887.1.2.7.54 holotype, 1* EtOH adult (female), 104 mm SL, Brazil; USNM 465413, 1′ CS larva (sex undetermined), 24.1 mm SL, Florida; USNM 204354, 1 EtOH adult (male), 161 mm SL, French Guiana; USNM 383908, 1 EtOH adult (male), 162 mm SL, North Carolina; USNM 395813, 2 CS adult (male and female) 158–181 mm SL, Alabama; USNM 407635, 1*′ EtOH adult (female), 197 mm SL, Guatemala; USNM 455509, 2 CS adult (male), 106–132 mm SL, Dominica; USNM 485813, 1 EtOH adult (male), 126 mm SL, Florida; USNM 485815, 1 EtOH adult (male), 184 mm SL, Nicaragua; USNM 485816, 1 EtOH adult (female), 198 mm SL, Alabama; USNM 485817, 1 EtOH adult (female), 190 mm SL, Mexico; USNM 485818, 1 EtOH adult (female), 120 mm SL, Alabama; USNM 485819, 1 EtOH adult (male), 155 mm SL, Mexico; USNM 485820, 1 EtOH adult (female), 161 mm SL Colombia; USNM 485821, 1 EtOH adult (male), 217 mm SL, Saba; USNM 485823, 2 EtOH adult (male and female), 170–175 mm SL, Belize; USNM 485824, 1 EtOH adult (female), 200 mm SL, Surinam; USNM 485825 1 EtOH adult (female), 172 mm SL, Florida; USNM 485826, 1 EtOH adult (male), 169 mm SL, Panama; USNM 485828, 1 EtOH adult (male), 159 mm SL, Louisiana; USNM 485830, 1 EtOH adult (female) 158 mm SL, Nicaragua. ***Diplacanthopoma kovacsi* sp. nov:** ZMH-ICH-0107333 holotype, 1* EtOH adult (male), 259 mm SL, Brazil; USNM 485829 paratype, 1 EtOH adult (female), 253 mm SL, Mexico; USNM 485842, paratype 1 EtOH adult (female), 207 mm SL, Mexico; USNM 465331, 1 CS larva (sex undetermined), 37.4 mm SL, Florida.

Genus *Diplacanthopoma* Günther, 1887

Type species: *Diplacanthopoma brachysoma* Günther, 1887, by monotypy.

Diagnosis: Scales absent from head, dorsal, and anal fins; prominent skin flap ending in a large pore above upper angle of opercle, near posttemporal; posterior infraorbital pores 2; large sensory pore on cheek (i.e., "*Diplacanthopoma*" pore); developed rakers on first gill arch 3–6; precaudal vertebrae 18–30; pectoral-fin rays 23–31.

Distribution and habitat: Distributed in all tropical and subtropical seas, bathydemersal at depths of about 200–1,700 m on upper continental slopes.

Species: 8 nominal species, many in need of revision, and several undescribed species.

***Diplacanthopoma kovacsi*, sp. nov.**

urn:lsid:zoobank.org:act:7D82825B-2C95-4DF1-8314-EC886EB96CDE

Figures 1–7

Holotype: ZMH-ICH-0107333 (formerly ISH 1920-1968), adult (male), 259 mm SL, 24°21'S, 43°54'W, 2 March 1968, 487 to 500 m, RV Walter Herwig 1, cruise 23, station 90/68, collected by G. Krefft.

Paratypes: USNM 485829, adult (female), 259 mm SL, 18°56'N, 94°26'W, 5 June 1970, 722 m, RV Oregon II, cruise 18, station 10962; USNM 485842, adult (female), 207 mm SL, 19°28'N, 92°55'W, 9 June 1970, 613 m, RV Oregon II, cruise 18, station 10984.

FIGURE 1. Holotype of *Diplacanthopoma kovacsi* **sp. nov.** ZMH-ICH-0107333, 259 mm SL. **A)** Left lateral view; **B)** dorsal view; **C)** ventral view. Scale bars = 5 cm.

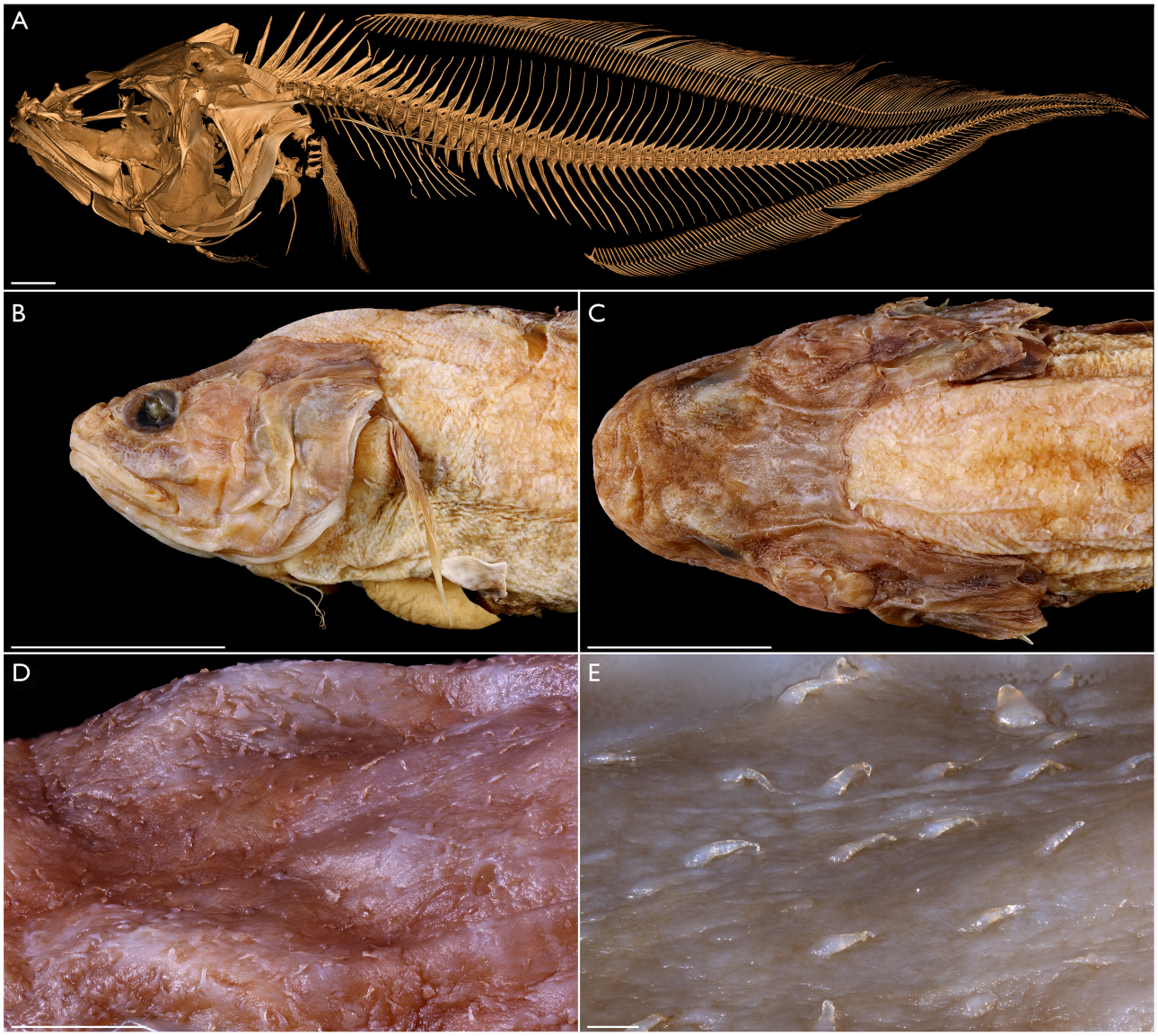

FIGURE 2. Internal osteology and head papillae of *Diplacanthopoma kovacsi* **sp. nov.** ZMH-ICH-0107333 holotype. **A)** µCT scan of whole body. Scale bar = 1 cm. **B)** Close-up lateral view of head to highlight papillae. Scale bar = 5 cm. **C)** Close-up dorsal view of head to highlight papillae. Scale bar = 5 cm. **D)** Close-up view of interorbital region to highlight papillae. Scale bar = 5 mm. **E)** Close-up view of papillae. Scale bar = 500 µm.

Larva: USNM 465331, sex undetermined, 37.4 mm SL, ~5 miles east of Lake Worth Inlet, Florida, 2 March 2021 (night), collected by S. Kovacs.

Diagnosis. Values and characters listed in brackets represent states for the only other Atlantic species, *D. brachysoma.* Precaudal vertebrae 20–23 [vs. 18–22]; total vertebrae 90–96 [vs. 75–94]; dorsal-fin rays 173–185 [vs. 125–164]; anal-fin rays 134–140 [vs. 88–127]; pectoral-fin rays 26–27 [vs. 22–26]; D/V = 7–8 [vs. 8–10]; D/A = 39–48 [vs. 34–44]; V/A = 26–29 [vs. 23–28]; HL:HD = 1.4–1.6 [vs. 1.7–2.0]; gill rakers on first arch 3 developed, 6–9 flattened platelets on lower arch, 2–3 platelets on upper arch [vs. 3–6 developed, 8–12 rudiments on lower arch, 3–4 rudiments on upper arch]; papillae on occiput, snout, below eye, and lower jaw [vs. absent]; ethmoid spine moderately elongate, dull tip [vs. short, sharp, often recurved tip]; frontal expanded laterally, interorbital broad [vs. not expanded, interorbital narrow]; frontal with lamellar bone extending above orbit [vs. reduced to absent], dermal integuments along central portion of lower lip [vs. absent]; OL:OH = 2.1 [vs. 1.8–2.1]; OL:TCL = 1.85 [vs. 1.85–2.15]; TCL:TCH = 1.45 [vs. 2.9–3.5].

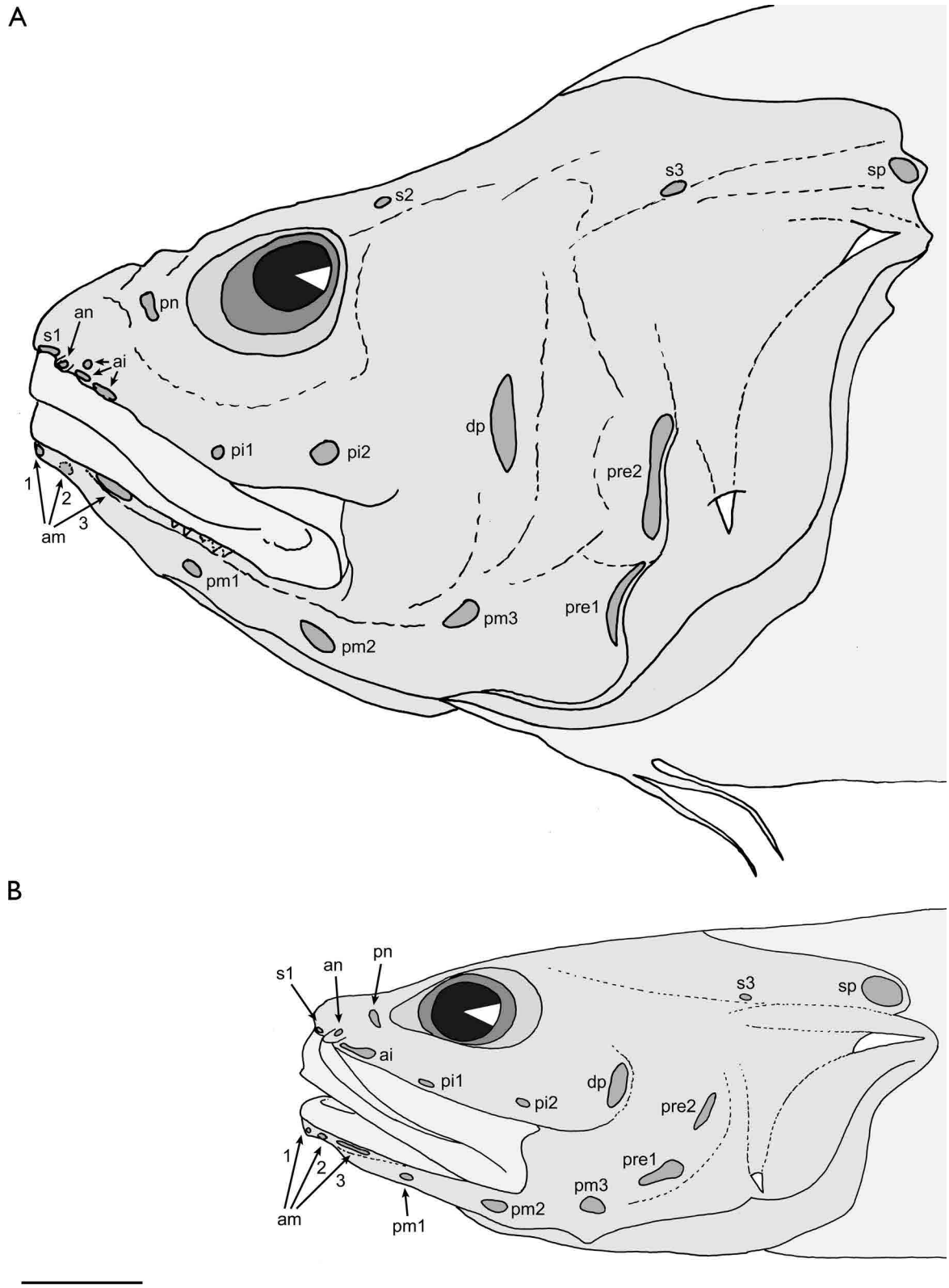

FIGURE 3. Sensory head pore systems of *Diplacanthopoma* from the western Atlantic. **A)** *Diplacanthopoma kovacsi* **sp. nov.** ZMH-ICH-0107333 holotype; **B)** *Diplacanthopoma brachysoma* USNM 464041. Abbreviations used: **an** = anterior nostril; **pn** = posterior nostril; **s1**, **s2**, **s3** = supraorbital-canal pores numbered from anterior to posterior; **sp** = posterior supraorbital-canal pore; **ai** = anterior infraorbital-canal pores (not numbered due to being highly variable); **pi1**, **pi2** = posterior infraorbital-canal pores; **dp** = "*Diplacanthopoma*" pore; **am1**, **am2**, **am3** = anterior mandibular-canal pores numbered from anterior to posterior (**am2** projected, not seen from lateral view); **pm1**, **pm2**, **pm3** = posterior mandibular-canal pores numbered from anterior to posterior; **pre1**, **pre2** = preopercular pores numbered from ventral to dorsal. Scale bars = 1 cm.

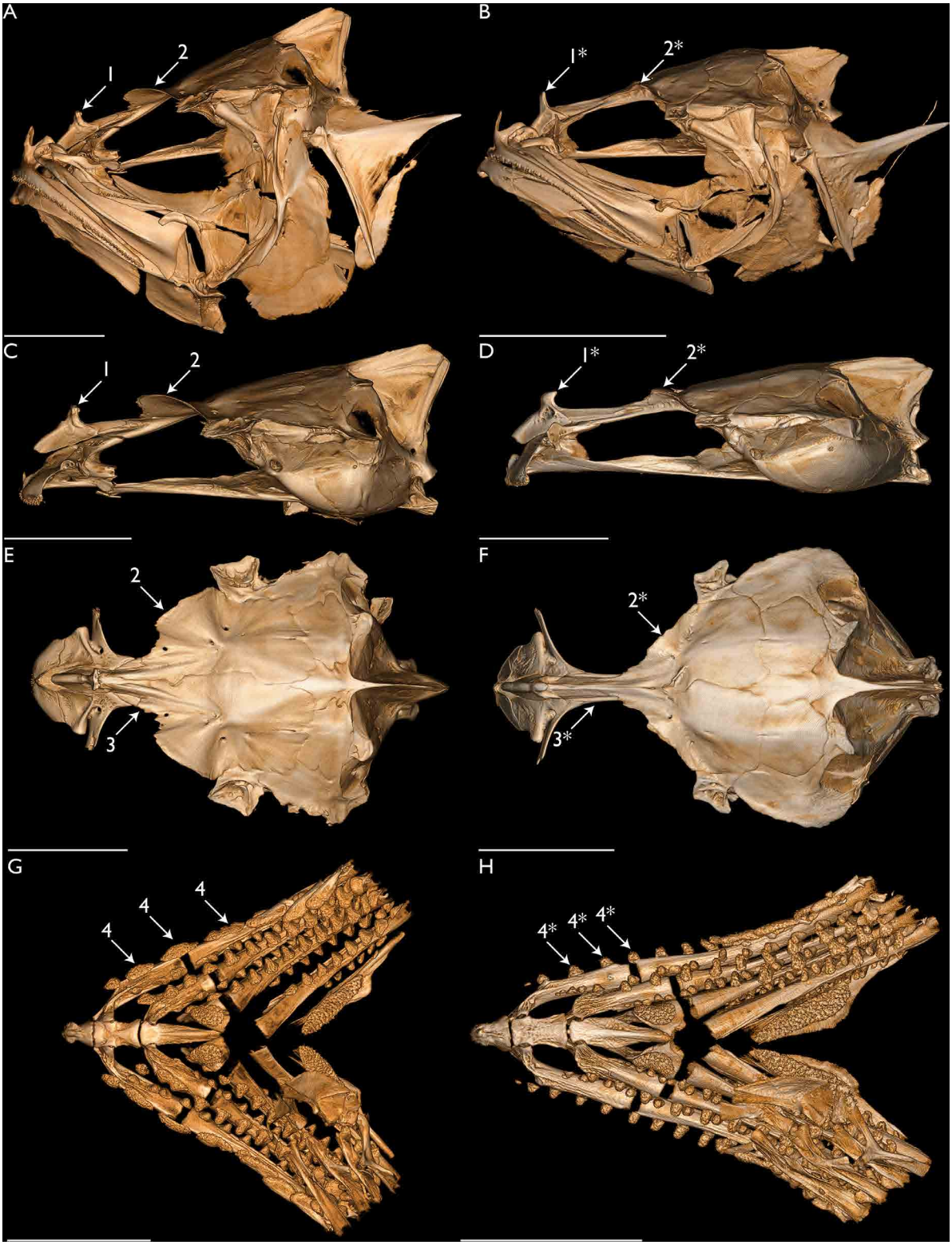

FIGURE 4. Osteological characters differentiating *Diplacanthopoma kovacsi* **sp. nov.** from *D. brachysoma*. **A**, **C**, **E, G**) *D. kovacsi* **sp. nov.** ZMH-ICH-0107333 Holotype. **B**) *D. brachysoma* BMNH 1887.1.2.7.54 holotype. **D**, **F, H**) *D. brachysoma* USNM 407635. A and B = lateral view of neurocranium, suspensorium, and oral jaws; C and D = lateral view of isolated neurocranium; E and F = dorsal view of neurocranium; G and H = dorsal view of branchial basket. 1 = ethmoid spine elongate, dull tipped. 1* = ethmoid spine short, tip often recurved with point. 2 = frontal with lamellar bone extending above orbit. 2* = frontal with reduced or without lamellar bone extending above orbit. 3 = interorbital region of frontal broad. 3* = interorbital region of frontal narrow. 4 = undeveloped gill rakers as flat platelets. 4* = undeveloped gill rakers as rounded rudiments. Scale bars = 1 cm.

TABLE 1. Counts and measurements for *Diplacanthopoma brachysoma* and *D. kovacsi*.

	Diplacanthopoma kovacsi N=4* (Holotype)	*Diplacanthopoma brachysoma* N=25* (Holotype)
SL (mm)	37.4–259 (259)	24.1–217 (104)
Counts		
Precaudal vertebrae	20–23 (21)	18–22 (21)
Caudal vertebrae	67–75 (75)	55–75 (55)
Total vertebrae	90–96 (96)	75–94 (76)
Dorsal-fin rays	173–185 (179)	125–164 (132)
Anal-fin rays	134–140 (136)	88–127 (98)
Pectoral-fin rays	26–27 (26–27)	22–26 (24)
Pelvic-fin rays	2 (2)	2 (2)
Caudal-fin rays	9–10 (9)	8–10 (8)
D/V	7–8 (8)	8–10 (8)
D/A	39–48 (48)	34–44 (36)
V/A	26–29 (29)	23–28 (25)
Total gill rakers	11–15 (11)	17–22 (18)
Developed gill rakers	3 (3)	3–6 (3)
Measurements (% of SL)		
HL	26.4–27.6 (27.6)	22.0–25.3 (23.4)
HW	15.9–17.9 (17.9)	12.0–15.6 (12.3)
HD	17.0–19.5 (19.5)	11.2–13.8 (13.8)
HL:HD	1.4–1.6 (1.4)	1.7–2.0 (1.7)
Max body depth	17.0–23.3 (21.8)	11.2–19.1 (18.6)
Body depth at anal-fin origin	12.3–19.1 (19.1)	9.2–11.9 (11.9)
Snout length	4.9–6.0 (4.9)	3.9–4.8 (4.7)
Upper-jaw length	11.3–12.0 (11.5)	9.6–11.8 (11.0)
Interorbital width	6.5–7.2 (7.2)	2.4–4.0 (2.4)
Orbital diameter	4.5–4.6 (4.5)	4.4–5.5 (5.3)
Pupil diameter	2.1–2.4 (2.1)	2.2–3.2 (2.6)
Pectoral-fin length	13.8–15.0 (14.7)	11.2–14.0 (Damaged)
Dentition		
Upper jaw	4–6 rows small teeth	4–6 rows small teeth
Vomer	Broad, triangular	Broad, triangular
Palatine	3–4 rows small teeth	3–4 rows small teeth
Dentary	4–5 rows small teeth	4–5 rows small teeth
Basihyal	Absent	Absent
Basibranchial 1–4	Absent	Absent
Hypobranchial 3	Present	Present
Undeveloped gill-raker shape	Flat platelets	Rounded rudiments
Sensory pores		
Supraorbital	4	4
Anterior infraorbital	3	2
Posterior infraorbital	2	2
"*Diplacanthopoma*" pore	Large	Large
Anterior mandibular	3	3

.....continued on the next page

TABLE 1. (Continued)

	Diplacanthopoma kovacsi N=4* (Holotype)	*Diplacanthopoma brachysoma* N=25* (Holotype)
Posterior mandibular	3	3
Preopercular	2, large	2, moderate
Ethmoid spine	Elongate, dull tipped	Short, tip often recurved
Opercular spine(s)	2 free, strong	2 free, strong
Head papillae	Occiput, snout, below eye, few on mandible	Absent
Otolith	N=1 (Holotype)	N=6
OL:OH	2.1	1.8–2.1
OH:OT	1.6	1.9–2.2
OL:TCL	1.85	1.85–2.15
TCL:TCH	1.45	2.9–3.5

Remarks. See in-text abbreviation section for abbreviations. *Larval specimens only included in counts, where possible.

Adult description. Compact species with large head, short, robust snout, and tapering tail (Figs. 1–2). Head naked, broad, high and relatively short, with distinctly concave dorsal profile. Many 1–2 mm long papillae (Fig. 2) on occiput, snout, below eye, and few on mandible; dermal integuments along central portion of lower lip. Opercle with 2 sharp, strong, extruding spines, upper one horizontal, lower one nearly vertical ventrally (Fig. 4). Eye and orbit relatively small, orbit diameter subequal to snout length. Maxilla extending posterior to vertical at posterior margin of eye, strongly widened posteriorly, rear part partly covered by thick skin. Anterior nostril small, positioned in short, fleshy tube low on snout; posterior nostril wide, anterior to lower margin of orbit. Body scaled, including regions immediately behind head and surrounding pelvic fins; scales cycloid.

Sensory pores (Fig. 3): Supraorbital-canal pores 4, 1st on tip of snout, 2nd above and behind eye, 3rd above commencement of opercle, 4th (large) in broad skin flap above opercular spine. Infraorbital-canal pores 5, anterior pores 3, 2 in skin flap of upper lip, with small pore above, and posterior pores 2, positioned on upper lip distantly spaced from anterior infraorbital pores. Large "*Diplacanthopoma*" pore on rear central position on cheek. Mandibular-canal pores 6, anterior pores 3, 1st at tip of lower jaw, 2nd (large) inside tip of lower jaw, 3rd (slit-like) in skinfold below lower lip, and posterior pores 3, set at subequal distances curving around lower mandible. Preopercular pores 2 (large) along rear skinfold over preopercle. A comparative drawing of the sensory head pores of *D. brachysoma* is also shown on Figure 3. Lateral-line origin immediately posterior to upper edge of opercle, running parallel to dorsal-fin base, becoming inconspicuous slightly before vertical through origin of anal fin. Lateral line noticeably darker on flank. Individual pores unable to be reliably counted.

Dentition. All teeth small, uniform (Fig. 4). Vomer broad, triangular; palatine long, with 3–4 rows of small teeth; premaxilla tooth patch not fused to adjacent premaxilla anteriorly, with 4–5 rows of small teeth; dentary tooth patch not fused to adjacent dentary anteriorly, with 4–5 rows of small teeth. Basihyal and basibranchial tooth plates absent (Fig. 4). Hypobranchial 3 tooth plate present.

Otolith morphology (Fig. 5; based on holotype). Size 10.1 mm in length; OL:OH = 2.1; OH:OT = 1.6. Thick, elongate, droplet-shaped otolith, anteriorly broadly rounded, posteriorly tapering. Dorsal rim highest anteriorly, overall shallow with long, straight central portion and weak, rounded post-dorsal angle near posterior tip of otolith. Ventral rim shallow, regularly curved. All rims smooth. Inner face completely flat with large, centrally positioned sulcus. Sulcus margins indistinct but single, large colliculum somewhat elevated and clearly discernable (used for measurements as total colliculum = TC), OL:TCL = 1.85. Colliculum wide, TCL:TCH = 1.45. Ventral margin of colliculum more strongly curved than dorsal margin. Dorsal and ventral fields smooth, narrow, without dorsal depression or ventral furrow. Outer face convex, smooth. Illustration of the otoliths from the Atlantic congener, *D. brachysoma*, shown in Figure 5 for comparison. For further information about extant ophidiiform otoliths see Nolf (1980) and Schwarzhans (1981).

Coloration. Fresh-specimen coloration unknown. Color of preserved specimens light to medium brown; head slightly darker than body.

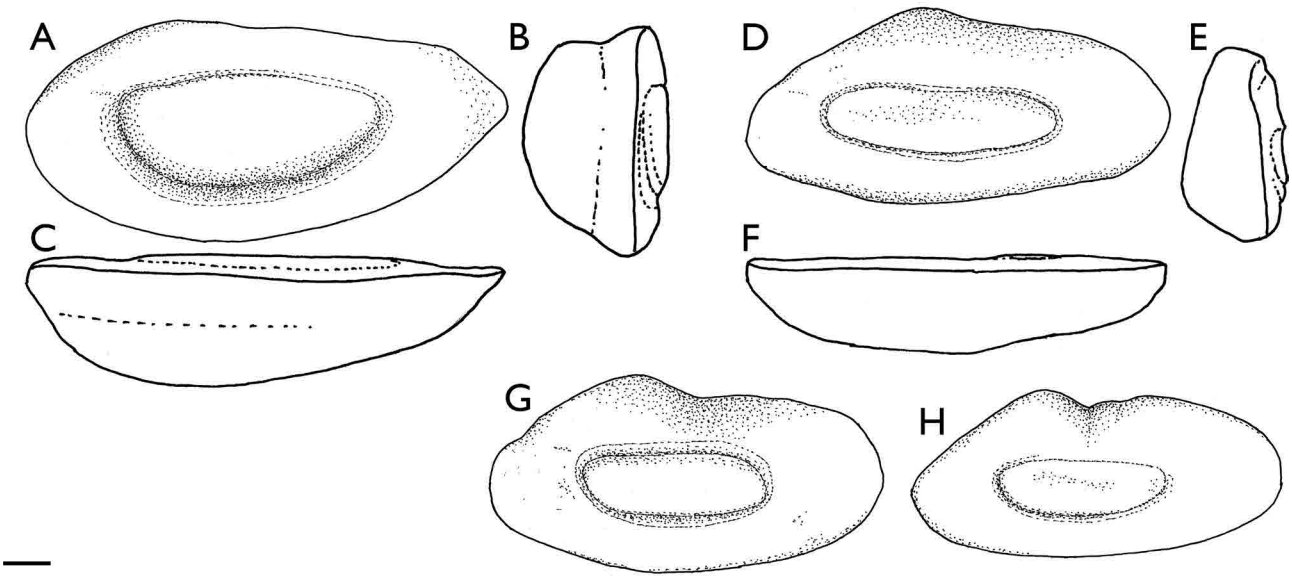

FIGURE 5. Otoliths of *Diplacanthopoma* from the western Atlantic. **A–C)** *Diplacanthopoma kovacsi* **sp. nov.** (holotype ZMH-ICH-0107333), A = inner face view, B = view from anterior, C = ventral view; **D–H)** *Diplacanthopoma brachysoma*, D, G, H = inner face views, E = view from anterior, F = ventral view, D–F = NSMT P-42409, G = USNM 485864, H = USNM 464040. Scale bar = 1 mm.

Larval description. USNM 465331 (Fig. 6), postflexion. Counts: dorsal-fin rays 184; anal-fin rays 140; pectoral-fin rays undifferentiated; precaudal vertebrae 23, total vertebrae 90. Following description based on *in-situ* images as well as on observations of an ethanol-preserved, cleared-and-stained specimen. Head large, nearly as deep as long. Body elongate. Maxilla and premaxilla short, at oblique upturned angle. Premaxilla and dentary with small, distantly spaced teeth. Distal end of maxilla dorsoventrally expanded, posterior margin convex. Supramaxilla indistinguishable. Large rostral cartilage attached to ascending process of premaxilla. Short spine associated with symphysis of dentary. Eight branchiostegals (full complement). Three elongate gill rakers present on first arch. Other tooth plates of branchial arches not developed. Body and head scaleless. Pectoral fin small, radials and fin rays undifferentiated. Coracoid with elongate cartilaginous ventral process, extending to level of anterior gut. Gut large, lacking exterilium morphology of some other larval ophidiids (Fraser & Smith 1974; Fahay & Nielsen 2003; Okiyama 2014; Girard *et al.* 2023b). Gut with single, broad intestinal loop in posterior half of tract, near the 14th–15th vertebra. Anus slightly anterior to anal fin. Pelvic fin indistinguishable. Caudal fin small, with ~10 rays; without procurrent rays, medial rays longest. Hypurals undifferentiated.

Melanophores absent from oral jaws. Melanophores present above frontal, along dorsal and ventral edges of body, minute. Body almost completely transparent. Fine, dense areas of reflectance or iridescence covering dorsal part of head, dorsal, anal, and caudal fins. These areas not discernible in preserved specimen. Melanophores dorsal to gut more pronounced than body melanophores.

Etymology. Named for blackwater SCUBA diver and photographer Steven Kovacs for his dedication to the discovery, photography, collection, and identification of larval fishes.

Distribution. The holotype was collected off the continental margin on the slope off southern Brazil, whereas the paratypes were collected off Tabasco and Veracruz, Mexico, in the Bay of Campeche (Fig. 7). Although the larva was collected off the eastern coast of Florida, we have not identified an adult specimen of this species from north of the Bay of Campeche. *Diplacanthopoma kovacsi* is sympatric with *D. brachysoma* for at least the southern part of the range of *D. brachysoma*.

Genotypic data. The barcode sequence from the larva (USNM 465331: GenBank Nucleotide PZ298824) was compared to sequences from adult and larval specimens of *Diplacanthopoma brachysoma* (USNM 407635: GenBank Nucleotide PZ298825; USNM 465413: GenBank Nucleotide PZ298823) and was found to be ≥9% divergent.

FIGURE 6. Blackwater and specimen photos of larval *Diplacanthopoma kovacsi* **sp. nov.** USNM 465331. Top three photos © S. Kovacs; *in-situ* specimen photographed and captured off West Palm Beach, Florida, 2 March 2021 (night). *In-situ* photos not to scale. Bottom photo of preserved specimen prior to clearing and staining. Scale bar = 1 mm.

Larval description of *D. brachysoma*. USNM 465413 (Fig. 8), postflexion. Counts: dorsal-fin rays 146; anal-fin rays 106; pectoral-fin rays undifferentiated; precaudal vertebrae 21, total vertebrae 83. Following description based on *in-situ* images as well as ethanol and cleared-and-stained specimen. Head large, nearly as deep as long. Body elongate. Maxilla and premaxilla short, at oblique upturned angle. Premaxilla and dentary with small, distantly spaced teeth. Distal end of maxilla dorsoventrally expanded, posterior margin convex. Supramaxilla indistinguishable. Large rostral cartilage attached to ascending process of premaxilla. Eight branchiostegals (full complement). Gill rakers and other tooth plates of branchial arches not developed. Body and head scaleless. Pectoral fin small, radials and fin rays undifferentiated. Coracoid with elongate cartilaginous ventral process, extending to level of anterior gut. Gut large, lacking exterilium morphology of some other larval ophidiids (Fraser & Smith 1974; Fahay & Nielsen 2003; Okiyama 2014; Girard *et al.* 2023b). Gut with single, broad intestinal loop in posterior half of tract, near the 13th-to-14th vertebra. Anus slightly anterior to anal fin. Pelvic fin indistinguishable. Caudal fin small, rays undifferentiated. Hypurals undifferentiated.

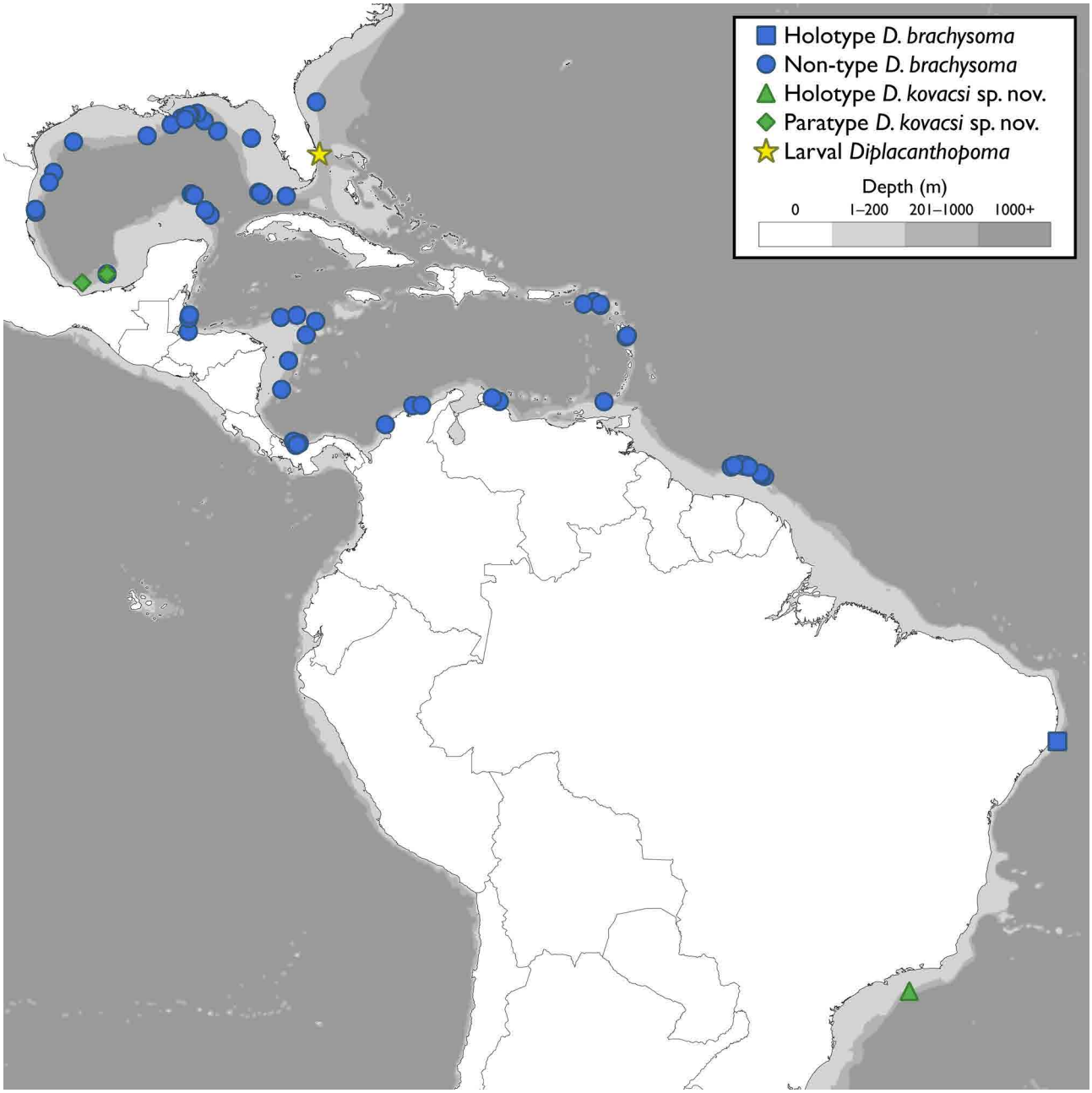

FIGURE 7. Distribution of *Diplacanthopoma* in the western Atlantic based on larval and adult specimens examined in this study. Coordinates based on specimens in Supplementary S1.

Melanophores absent from oral jaws, frontal, and along dorsal of body until ~18th vertebra. Melanophores present in dense band dorsally from 18th vertebra to caudal fin and ventrally from anal-fin origin to caudal fin. Body almost completely transparent. Band of yellow reflectance or iridescence below vertebrae from head to caudal fin. Blotches of yellow reflectance or iridescence along anal fin. It is unclear if this area is yellow in life or the result of strobes used in photography. Minute areas of white reflectance or iridescence along dorsal fin and dorsal part of head. These areas not discernible in preserved specimen. Melanophores dorsal to gut present in dense band, with greatest density above gut loop.

Genotypic data. The barcode sequence from the larva (USNM 465413: GenBank Nucleotide PZ298823) was compared to a sequence from an adult specimen of *D. brachysoma* (USNM 407635: GenBank Nucleotide PZ298825) and was 99.7% identical, differing by 2 base pairs.

Discussion

Specimens of bythitids are seemingly rare in collections of larval fishes, possibly due to their unremarkable traits and/or lack of well-defined characteristics. With their elongate bodies, lack of markedly elongate dorsal-, anal-, and pectoral-fin rays, and inconspicuous pigmentation, the larvae of *Diplacanthopoma* are reminiscent of elongate larval ophidiids, such as *Ophidion, Lepophidium*, and *Otophidium*, that can be found in the western Atlantic (e.g., Richards 2005; Fahay 2007). In addition to differences in fin-ray and myomere counts, larval specimens of *Ophidion, Lepophidium*, *Otophidium,* and similar ophidiids can be distinguished from the larvae of *Diplacanthopoma* based on length of the gut and gut morphology. The position of the tightly looped gut in larval ophidiids can be used for species-specific identifications (Fahay 2007). Comparatively, the gut in larval *Diplacanthopoma* is broad and elongate. Although the gut loop in *Diplacanthopoma* is in the posterior half of the tract, similar to *Ophidion nocomis* and *Ophidion selenops* (Fahay 2007), the gut loop in *Diplacanthopoma* is broad and posteriorly displaced. Pigmentation associated with the gut also differs, with pigmentation often concentrated near the gut loop or ventral to the gut in some species of ophidiid compared to broadly distributed and variously dense melanophores associated with the elongate gut in *Diplacanthopoma*.

FIGURE 8. Blackwater and specimen photos of larval *Diplacanthopoma brachysoma* USNM 465413. Top two photos © D. Devers; *in-situ* specimen photographed and captured off West Palm Beach, Florida, 4 May 2022 (night). *In-situ* photos not to scale. Bottom photo of preserved specimen prior to clearing and staining. Scale bar = 1 mm.

Diplacanthopoma kovacsi differs from the only other Atlantic congener, *D. brachysoma*, in the following characters (values and characters for *D. brachysoma* in parentheses). Counts: dorsal-fin rays 173–185 (vs. 125–164), anal-fin rays 134–140 (vs. 88–127). Measurements: HD 17.0–19.5% of SL (vs. 11.2–13.8), body depth at anal-fin origin 12.3–19.1 (vs. 9.2–11.9), interorbital width 6.5–7.2 (vs. 2.4–4.0). Skull morphology from μCT scans: frontal with lamellar bone extending above orbit (vs. with reduced or without lamellar bone extending above orbit), interorbital region of frontal broad (vs. narrow). Additionally, there are differences in the shapes of certain bones or articulations in the neurocranium and suspensorium between the two species (Fig. 4). We refrain from describing these differences in detail until osteological information can be collected from additional species of *Diplacanthopoma.* Otolith: OH:OT 1.6 (vs. 1.9–2.2), TCL:TCH 1.45 (vs. 2.9–3.5). The otolith of the holotype of *D. kovacsi* differs further from that of *D. brachysoma* in its drop-like shape with a tapering posterior tip, versus nearly symmetrical shape with a slightly elevated predorsal lobe, middorsal depression, and a rounded posterior tip in *D. brachysoma*. Differences were also detected in gill-raker morphology, with gill rakers flattened into platelets on lower and upper arches in *D. kovacsi* versus more-developed rudiments in all specimens of *D. brachysoma* examined. As specimens of *D. brachysoma* are considerably smaller than those of *D. kovacsi* examined in this study, it is unclear if these differences in gill-raker morphology are diagnostic to the species or the result of ontogeny. Identification of comparatively larger specimens of *D. brachysoma* or smaller *D. kovacsi* will provide needed context to evaluate the differences we observe in gill-raker morphology. Additionally, *D. kovacsi* shows many 1–2 mm long papillae on the head, particularly on the snout, around the eye and less commonly on the occiput and the lower jaw, with dermal integuments along the central portion of the lower lip, all of which have not been observed in *D. brachysoma*.

We have not identified an adult specimen of *D. kovacsi* from north of the Bay of Campeche. It is unclear if this new taxon is more broadly distributed throughout the western Atlantic, similar to *D. brachysoma*, or if the larva of *D. kovacsi* captured in Florida was transported by currents farther north to Floridian waters; particularly as Nonaka *et al.* (2021) found and blackwater divers have captured (unpublished) some Southwest Atlantic species in the blackwater of Florida. Based on adult specimens examined, *D. kovacsi* overlaps in geographic distribution with *D. brachysoma* (Fig. 7), with paratype specimens caught in the same localities within the Bay of Campeche as *D. brachysoma*. The two species also overlap in depth of capture, although specimens of the new species are limited by comparison to *D. brachysoma*.

Relationships between the two western Atlantic species of *Diplacanthopoma* were not assessed in this study. Relationships have not been proposed among species of *Diplacanthopoma* broadly, likely due to the genus needing revision; including the species found in the Indian and Pacific Oceans. Further, delimiting species and understanding relationships among *Diplacanthopoma* continues to present challenges. Echoing the concerns raised by Cohen & Nielsen (2002), many of the specimens examined in this study sustained damage to their tails prior to capture and/or preservation. Subsequent works on the taxonomy and systematics of *Diplacanthopoma* must account for these anomalous specimens and look to other characters, such as internal osteological differences (Figs. 4 and 5), to delimit species.

Acknowledgements

We thank blackwater divers and photographers R. Collins, A. Deloach, N. Deloach, D. Devers, C. Guglielmo, L. Ianniello, J. Milisen, R. Minemizu, S. Kovacs, M. Rivera, and A. Whitaker for documenting larval fishes and contributing to the USNM collections. The lead author thanks G.D. Johnson [deceased] and A. Nonaka (USNM) for the many conversations about larval fishes and for their encouragement. We also thank J. Maclaine (BMNH), B. Clark and A. Lanzetti (Micro-CT laboratory of the Natural History Museum, London), T. Weddehage and K. Engelkes (LIB), and J.J. Hill (NMNH) for assistance with μCT scanning; J. Williams (USNM) and G. Shinohara (NSMT) for facilitating otolith extraction of figured specimens; A. Nonaka (USNM) for performing DNA sequencing; J. Maclaine (BMNH), A. Reft and L. Willis (National Systematics Lab, National Oceanic and Atmospheric Administration), C. Baldwin, A. Harvey, K. Murphy, L. Parenti, and D. Pitassy (USNM) for providing support and/or access to specimens in their care. Extractions and sequencing of DNA were conducted at the NMNH Laboratories of Analytical Biology.

Data availability

The data generated and/or analyzed in this article are available on MorphoSource or GenBank.

Declarations

Conflicts of interest. The authors declare no conflicts of interest.

Ethics approval. Species of fishes in this study are not listed as threatened or endangered by the IUCN Red List or CITES. All methods of capture and preservation conform to the Guidelines for the Use of Fishes in Research established by the American Fisheries Society, American Institute of Fishery Research Biologists, and American Society of Ichthyologists and Herpetologists. Larvae were acquired under Florida permit SAL-21-2155A-SR.

References

Afonso, G.V.F., Johnson, G.D., Collins, R. & Pastana, M.N.L. (2025) Associations between fishes (Actinopterygii: Teleostei) and anthozoans (Anthozoa: Hexacorallia) in epipelagic waters based on in situ records. *Journal of Fish Biology*, 107 (6), 2166–2172.
https://doi.org/10.1111/jfb.70214

Baldwin, C.C., Mounts, J.H., Smith, D.G. & Weigt, L.A. (2009) Genetic identification and color descriptions of early life-history stages of Belizean *Phaeoptyx* and *Astrapogon* (Teleostei: Apogonidae) with comments on identification of adult *Phaeoptyx*. *Zootaxa*, 2008 (1), 1–22.
https://doi.org/10.11646/zootaxa.2008.1.1

Cohen, D.M. & Haedrich, R.L. (1983) The fish fauna of the Galapagos thermal vent region. *Deep Sea Research Part A. Oceanic Research Papers*, 30 (4), 371–379.
https://doi.org/10.1016/0198-0149(83)90072-9

Cohen, D.M. & Nielsen, J. (2002) *Diplacanthopoma kreffti* (Pisces, Bythitidae), a new species from the Northwest Australian shelf, with comments on the name *D. alcockii* Goode and Bean, 1896. *Archive of Fishery and Marine Research*, 50 (1), 11–15.

Fahay, M.P. (2007) *Early Stages of Fishes in the Western North Atlantic Ocean (Davis Strait, Southern Greenland and Flemish Cap to Cape Hatteras)*. Northwest Atlantic Fisheries Organization, Dartmouth, Nova Scotia, 1696 pp.

Fahay, M.P. & Nielsen, J. (2003) Ontogenetic evidence supporting a relationship between *Brotulotaenia* and *Lamprogrammus* (Ophidiiformes: Ophidiidae) based on the morphology of exterilium and rubaniform larvae. *Ichthyological Research*, 50 (3), 209–220.
https://doi.org/10.1007/s10228-003-0159-5

Fedorov, A., Beichel, R., Kalpathy-Cramer, J., Finet, J., Fillion-Robin, J.-C., Pujol, S., Bauer, C., Jennings, D., Fennessy, F., Sonka, M., Buatti, J., Aylward, S., Miller, J.V., Pieper, S. & Kikinis, R. (2012) 3D Slicer as an image computing platform for the Quantitative Imaging Network. *Magnetic Resonance Imaging*, 30 (9), 1323–1341.
https://doi.org/10.1016/j.mri.2012.05.001

Fraser, T.H. & Smith, M.M. (1974) An exterilium larval fish from South Africa with comments on its classification. *Copeia*, 1974 (4), 886–892.
https://doi.org/10.2307/1442587

Fricke, R., Eschmeyer, W.N. & Van der Laan, R. (Eds.) (2025) Eschmeyer's Catalog of Fishes: Genera, Species, References. Available from: http://researcharchive.calacademy.org/research/ichthyology/catalog/fishcatmain.asp (accessed 15 December 2025)

GBIF.org (2025) GBIF Occurrence Download. Available from: https://doi.org/10.15468/dl.vwpwda (accessed 15 December 2025)

Girard, M.G., Carter, H.J. & Johnson, G.D. (2023a) New species of *Monomitopus* (Ophidiidae) from Hawai'i, with the description of a larval coiling behavior. *Zootaxa*, 5330 (2), 265–279.
https://doi.org/10.11646/zootaxa.5330.2.5

Girard, M.G., Davis, M.P. & Smith, W.L. (2020) The phylogeny of carangiform fishes: morphological and genomic investigations of a new fish clade. *Copeia*, 108 (2), 265–298.
https://doi.org/10.1643/ci-19-320

Girard, M.G., Davis, M.P., Tan, H.H., Wedd, D.J., Chakrabarty, P., Ludt, W.B., Summers, A.P. & Smith, W.L. (2022) Phylogenetics of archerfishes (Toxotidae) and evolution of the toxotid shooting apparatus. *Integrative Organismal Biology*, 4 (1), obac013.
https://doi.org/10.1093/iob/obac013

Girard, M.G., Mundy, B.C., Nonaka, A. & Johnson, G.D. (2023b) Cusk-eel confusion: revisions of larval *Luciobrotula* and

Pycnocraspedum and re-descriptions of two bythitid larvae (Ophidiiformes). *Ichthyological Research*, 70 (4), 474–489. https://doi.org/10.1007/s10228-023-00906-4

Girard, M.G., Nonaka, A., Baldwin, C.C. & Johnson, G.D. (2024) Discovery and description of elaborate larval cusk-eels and the relationships among *Acanthonus*, *Tauredophidium* and *Xyelacyba* (Teleostei: Ophidiidae). *NOAA Professional Paper NMFS*, 24, 20–42. https://doi.org/10.7755/pp.24.3

Goode, G.B. & Bean, T.H. (1896) *Oceanic Ichthyology: A Treatise on the Deep-sea and Pelagic Fishes of the World, Based Chiefly upon the Collections Made by the Steamers Blake, Albatross, and Fishhawk in the Northwestern Atlantic, with an Atlas Containing 417 Figures*. Government Printing Office, Washington, 553 pp. https://doi.org/10.5962/bhl.title.48521

Gosline, W.A. (1954) Fishes killed by the 1950 eruption of Mauna Loa II. Brotulidae. *Pacific Science*, 8, 68–83.

Günther, A. (1887) Report on the deep-sea fishes collected by H. M. S. Challenger during the years 1873–76. *In*: Thomson, C.W. & Murray, J. (Eds.), *Report on the Scientific Results of the Voyage of H. M. S. Challenger during the Years 1873–76. Zoology–Vol. XXII.* Eyre & Spottiswoode, London, pp. i–lx + 1–335. https://doi.org/10.5962/bhl.title.15693

Johnson, G.D., Collins, R.A. & Brothers, E.B. (2025) Putative Batesian mimicry of gelatinous zooplankton by larvae of marine fishes: a closer look based on in-situ images by blackwater photographers. *Journal of the Ocean Science Foundation*, 42, 91–119. https://doi.org/10.5281/zenodo.14889573

Kearse, M., Moir, R., Wilson, A., Stones-Havas, S., Cheung, M., Sturrock, S., Buxton, S., Cooper, A., Markowitz, S., Duran, C., Thierer, T., Ashton, B., Meintjes, P. & Drummond, A. (2012) Geneious Basic: an integrated and extendable desktop software platform for the organization and analysis of sequence data. *Bioinformatics*, 28 (12), 1647–1649. https://doi.org/10.1093/bioinformatics/bts199

Machida, Y. (1988) An additional specimen of imperfectly known bythitid fish, *Diplacanthopoma japonicum* (Bythitidae, Ophidiiformes). *Reports of the Usa Marine Biological Institute, Kochi University*, (10), 69–73.

Nielsen, J.G., Cohen, D.M., Markle, D.F. & Robins, C.R. (1999) Ophidiiform fishes of the world (order Ophidiiformes). *FAO Species Catalogue*, 18, 1–178.

Nolf, D. (1980) Etude monographique des otolithes des Ophidiiformes actuels et revision des especes fossiles (Pisces, Teleostei). *Mededelingen van de Werkgroep voor Tertiaire en Kwartaire Geologie*, 17 (2), 71–195.

Nonaka, A., Milisen, J.W., Mundy, B.C. & Johnson, G.D. (2021) Blackwater diving: an exciting window into the planktonic arena and its potential to enhance the quality of larval fish collections. *Ichthyology & Herpetology*, 109 (1), 138–156. https://doi.org/10.1643/i2019318

Okiyama, M. (Ed.) (2014) *An Atlas of Early Stage Fishes in Japan. 2nd Edition*. Tokai University Press, Tokyo, 1154 pp.

Pastana, M.N.L., Girard, M.G., Bartick, M.I. & Johnson, G.D. (2022) A novel association between larval and juvenile *Erythrocles schlegelii* (Teleostei: Emmelichthyidae) and pelagic tunicates. *Ichthyology & Herpetology*, 110 (4), 675–679. https://doi.org/10.1643/i2022008

Potthoff, T. (1984) Clearing and staining techniques. *In*: Moser, H.G., Richards, W.J., Cohen, D.M., Fahay, M.P., Kendall, Jr., A.W. & Richardson, S.L. (Eds.), *Ontogeny and Systematics of Fishes*. The American Society of Ichthyologists and Herpetologists, Lawrence, pp. 35–37.

Richards, W.J. (Ed.) (2005) *Early Stages of Atlantic Fishes: An Identification Guide for the Western Central North Atlantic*. CRC Press, Boca Raton, Florida, 1312 pp.

Rolfe, S., Pieper, S., Porto, A., Diamond, K., Winchester, J., Shan, S., Kirveslahti, H., Boyer, D., Summers, A. & Maga, A.M. (2021) SlicerMorph: An open and extensible platform to retrieve, visualize and analyse 3D morphology. *Methods in Ecology and Evolution*, 12 (10), 1816–1825. https://doi.org/10.1111/2041-210x.13669

Sabaj, M.H. (2020) Codes for natural history collections in ichthyology and herpetology. *Copeia*, 108 (3), 593–669. https://doi.org/10.1643/asihcodons2020

Schwarzhans, W. (1981) Vergleichende morphologische Untersuchungen an rezenten und fossilen Otolithen der Ordnung Ophidiiformes. *Berliner Geowissenschaftliche Abhandlungen* (*A*), 32, 63–122.

Weigt, L.A., Driskell, A.C., Baldwin, C.C. & Ormos, A. (2012) DNA barcoding fishes. *In*: Kress, W.J. & Erickson, D.L. (Eds.), *DNA barcodes: Methods and Protocols*. Humana Press, New York, New York, pp. 109–126. https://doi.org/10.1007/978-1-61779-591-6_6

Supplementary Materials. The following supporting information can be downloaded at the DOI landing page of this paper:

Supplementary S1. Capture date and locality for specimens included in this study.